

Duality, Magnetic space group and their applications to quantum phases and phase transitions on bipartite lattices in several experimental systems

Jinwu Ye

Department of Physics, The Pennsylvania State University, University Park, PA, 16802

(Dated: October 29, 2018)

By using a dual vortex method, we study phases such as superfluid, solids, supersolids and quantum phase transitions in a unified scheme in extended boson Hubbard models at and slightly away from half filling on bipartite optical lattices such as honeycomb and square lattice. We also map out its global phase diagram at $T = 0$ of chemical potential versus the ratio of kinetic energy over the interaction. We stress the importance of the self-consistence condition on the saddle point structure of the dual gauge fields in the translational symmetry breaking insulating sides, especially in the charge density wave side. We find that in the translational symmetry breaking side, different kinds of supersolids are generic possible states slightly away from half filling. We propose a new kind of supersolid: valence bond supersolid (VB-SS). In this VB-SS, the density fluctuation at any site is very large indicating its superfluid nature, but the boson kinetic energies on bonds between two sites are given and break the lattice translational symmetries indicating its valence bound nature. We show that the quantum phase transitions from solids to supersolids driven by a chemical potential are in the same universality class as that from a Mott insulator to a superfluid, therefore have exact exponents $z = 2, \nu = 1/2, \eta = 0$ with a logarithmic correction. Comparisons with previous quantum Monte-Carlo (QMC) simulations on a square lattice are made. Implications on possible future QMC simulations in both bipartite lattices are given. All these phases and phase transitions can be potentially realized in ultra-cold atoms loaded on optical bipartite lattices. Then we apply our results to investigate the reentrant "superfluid" in a narrow region of coverages in the second layer of ${}^4\text{He}$ adsorbed on graphite and the low temperature phase diagram of Hydrogen physisorbed on Krypton-prelated graphite ($H_2/\text{Kr}/\text{graphite}$) near half filling. We suggest that ${}^4\text{He}$ and H_2 lattice supersolids maybe responsible for the experimental signals in the two systems. Finally, we suggest Cooper supersolid is repressible for the phase diagram of $La_{2-x}Ba_xCuO_4$ near $x = 1/8$.

I. INTRODUCTION.

The Boson Hubbard model with various kinds of interactions, on all kinds of lattices and at different filling factors is described by the following Hamiltonian¹:

$$H = -t \sum_{\langle ij \rangle} (b_i^\dagger b_j + h.c.) - \mu \sum_i n_i + \frac{U}{2} \sum_i n_i(n_i - 1) + V_1 \sum_{\langle ij \rangle} n_i n_j + V_2 \sum_{\langle\langle ik \rangle\rangle} n_i n_k + \dots \quad (1)$$

where $n_i = b_i^\dagger b_i$ is the boson density, t is the nearest neighbor hopping which is determined by the depth of the trapping potential at the preferred adsorption sites. U, V_1, V_2 are onsite, nearest neighbor (nn) and next nearest neighbor (nnn) interactions respectively, the \dots may include further neighbor interactions and possible ring-exchange interactions.

In the hard-core limit $U \rightarrow \infty$, due to the exact mapping between the boson operator and the spin $s = 1/2$ operator: $b_i^\dagger = S_i^+, b_i = S_i^-, n_i = S_i^z + 1/2$, the boson model Eqn.1 can be mapped to a "generalized" anisotropic $S = 1/2$ quantum Heisenberg model in an external magnetic field^{16,48}:

$$H = -2t \sum_{\langle ij \rangle} (S_i^x S_j^x + S_i^y S_j^y) + V_1 \sum_{\langle ij \rangle} S_i^z S_j^z + V_2 \sum_{\langle\langle ik \rangle\rangle} S_i^z S_k^z - h \sum_i S_i^z + \dots \quad (2)$$

where $h = \mu - 2V_1 - 2V_2$ for a square lattice and the \dots may include further neighbor interactions and ring-exchange interactions.

The model Eqn.1 with only the onsite interaction was first studied in Ref.¹. It was found that there is a second order superconductor to insulator transition at filling factor $f = 1$. The effects of long range Coulomb interactions on the transition was studied in^{2,3}. The duality transformation to the dual vortex picture at $f = n$ was performed in⁴ and is briefly reviewed in the appendix. Here, we only outline its essence to facilitate the duality transformation in the more general cases $f = p/q$ to be discussed in the next several paragraphs. In the direct boson picture, a vortex is a singularity in the boson wavefunction, so a boson wavefunction acquires a 2π phase when in encircles a vortex. In the dual vortex picture, a boson is a singularity in the vortex wavefunction, so a vortex wavefunction acquires a 2π phase when in encircles a boson. After performing the boson-vortex duality transformation, the authors in⁴ obtained a dual theory of Eqn.1 in term of the interacting vortices ψ hopping on the dual lattice subject to a fluctuating "dual" magnetic field". The average strength of the dual "magnetic field" A_μ through a dual plaquette is equal to the boson density $f = n$, because $2\pi n$ is equivalent to 0, so the average value can be simply taken to be zero. It is important to stress that the average density of bosons is the same in both the SF and the Mott insulating side, namely, it takes the integer n on both sides, so the average strength of the dual magnetic field can be taken as *zero* on both

side, then the fluctuations in the dual gauge field reflects the fluctuations of the boson density. In the continuum limit, just from the gauge invariance, the final effective theory in terms of the vortex order parameter ψ is just the scalar electrodynamics of the dual vortex ψ coupled to the fluctuating gauge field A_μ described by Eqn.A2. In the superfluid state $\langle \psi \rangle = 0$, the gauge field is gapless, while in the insulating state $\langle \psi \rangle \neq 0$, the gauge field acquires a mass due to the Higgs mechanism. This duality transformation has been confirmed by Quantum Monte- Carlo (QMC) in the first reference in⁴.

Obviously, it is important to study other commensurate filling factors $f = p/q$ (p, q are relative prime numbers), because in addition to the superfluid phase, many other phases such as charge density wave or valence bond solid can only appear when $q \geq 2$. So novel phase transitions such as SF to CDW or SF to VBS can be realized only in such cases. Recently, the dual vortex method (DVM) developed in⁴ was greatly expanded to study Eqn.1 on a square lattice just at such generic filling factors in⁵. It turns out that the DVM at $q \geq 2$ is much more involved than the simplest $q = 1$ case due to the crucial involvement of the non-commutative projective space group at $q \geq 2$. The general procedures are the following. After performing the similar charge-vortex duality transformation as in⁴, the authors in⁵ obtained a dual theory of Eqn.1 in term of the interacting vortices ψ_a hopping on the dual lattice subject to a fluctuating *dual* "magnetic field". The average strength of the dual "magnetic field" through a dual plaquette is equal to the boson density $f = p/q$. This is similar to the Hofstadter problem of electrons moving in a crystal lattice in the presence of a magnetic field^{6,7}. The projective representation of the space group (PSG) dictates that there are at least q -fold degenerate minima in the mean field energy spectrum (when $q = 1$, the PSG just reduces to the usual commutative space group). Near the superconductor to the insulator transition, the most important ψ_a fluctuations will be near these q minima which can be labeled as $\psi_l, l = 0, 1, \dots, q - 1$ which forms a q dimensional representation of the PSG. In the continuum limit, the final effective theory in terms of these q order parameters should be invariant under this PSG. In the superfluid state $\langle \psi_l \rangle = 0$ for every l , while in the insulating state $\langle \psi_l \rangle \neq 0$ for at least one l . In the insulating state, there must exist some kinds of charge density wave (CDW) or valence bond solid (VBS) states which may be stabilized by longer range interactions or possible ring exchange interactions included in Eqn.1. The CDW or VBS order parameter was constructed to be the most general *bilinear* and gauge invariant combinations of the ψ_l ⁵.

In a recent unpublished preprint¹⁰, the author studied all the possible phases and phase transitions in the EBHM *slightly away* from half filling $q = 2$ on bipartite lattices such as honeycomb and square lattice. It was found in¹⁰ that the dual vortex method at $d = 2$ can achieve many important results which are very diffi-

cult to achieve from the direct boson picture. Although square lattice has been studied by various analytic and numerical methods before, the boson Hubbard model on a honeycomb lattice was not studied in any details by both analytic and Quantum Monte-Carlo (QMC) methods before the preprint¹⁰. It is not a Bravais lattice, so may show some different properties than those in square lattice. Experimentally, the honeycomb lattice could also be easily realized in ultra-cold atomic experiments to be discussed in section II. The honeycomb lattice is also the relevant lattice for adatom adsorption on substrates to be discussed in section VIII. I found that a *supersolid* (SS) state *exists only away from half filling*. A supersolid in Eqn.1 is a state with both superfluid and solid order. A supersolid in Eqn.2 is defined as the simultaneous orderings of ferromagnet in the XY component (namely, $\langle b_i \rangle \neq 0$) and CDW in the Z component. Recently, by using the torsional oscillator measurement, a PSU's group lead by Chan observed a marked $1 \sim 2\%$ superfluid component even in bulk solid 4He at $\sim 0.2K$ ⁸. If this experimental observation indicates the existence of 4He supersolid remains controversial⁹. However, it was established by spin wave expansion¹² and quantum Monte-carlo (QMC)^{13,14,15} simulations that a supersolid state could exist in an extended boson Hubbard model (EBHM) with suitable lattice structures, filling factors, interaction ranges and strengths.

It was also explicitly pointed out in¹⁰ that the DVM developed in⁵ holds only in the superfluid (SF) and the valence bond solid (VBS) side where the saddle point of the dual gauge field can be taken as uniform, however, it fails in the charge density wave (CDW) side where the saddle point of the dual gauge field can *not* be taken as uniform anymore. So not only the fluctuations, but also the average values of the dual gauge fields are different on both sides. This is in sharp contrast to the superfluid to the Mott transition at and near $f = n$ described by Eqns.A2 and A4 in the appendix. As explained below Eqn.A2, the average density of bosons is the same in both the SF and the Mott insulating side, namely, it takes the integer n on both sides, so the average strength of the dual magnetic field can be taken as a uniform zero on both sides, of course, the fluctuations of the gauge field are completely different on both sides. However, in the CDW side which breaks the translational symmetry, special care is needed to choose a correct saddle point of the dual gauge field in the CDW side to make the theory self-consistent, so a different action is needed in the CDW side¹⁰. This paper is an expanded version of the unpublished preprint¹⁰. In this expanded version, (1) by pushing the DVM to slightly away from commensurate filling factors and (2) also extending the DVM explicitly to the lattice symmetry breaking CDW side by choosing the corresponding self-consistent saddle points of the dual gauge field, I will map out the global phase diagram of the EBHM on bipartite optical lattices such as honeycomb and square lattice at and near half filling and also investigate superfluid, solid, especially supersolids

and quantum phase transitions in the phase diagram in a *unified* scheme.

The DVM is a magnetic space group (MSG)⁵ symmetry-based approach which, in principle, can be used to classify all the possible phases and phase transitions after choosing correct saddle points for the dual gauge fields. But the question if a particular phase will appear or not as a ground state depends on the specific values of all the possible parameters in the EBHM in Eqn.1, so it can only be addressed by a microscopic approach such as Quantum Monte-Carlo (QMC) simulations. The DVM can guide the QMC to search for particular phases and phase transitions in a specific model. Finite size scalings in QMC in a specific microscopic model can be used to confirm the phases and the universality classes of phase transitions discovered by the DVM. The two methods are complementary to each other and both are needed to completely understand phases and phase transitions in Eqn.1.

The rest of the paper is organized as following, In section II, I will explicitly derive the generators of the magnetic space group (also called projective space group) for $q = 2$ in a honeycomb lattice, construct the effective actions which are invariant under this MSG, also write down both the charge density wave and the valence bond order parameters to characterize the symmetry breaking sides in the insulating regimes. In section III and IV, I will describe the phases and phase transitions driven by the competition of kinetic energy and repulsive potential energy in Fig. 4 (represented by the parameter r in Fig. 2 and Fig.3) along the horizontal axis at the commensurate fillings and the phases and phase transitions driven by the chemical potential μ along the vertical axis slightly away from the commensurate fillings in Ising and easy-plane limit respectively. We also stress that satisfying the self-consistent condition for the dual gauge field in the Ising limit is absolutely necessary to achieve correct answers in the CDW side. In section V, we study the EBHM in a square lattice and also discuss the still disputed so called deconfined quantum critical point in the easy-plane limit. In section VI, we compare our results achieved by the DVM with some available QMC results and make implications on possible future QMC simulations in both lattices. Then we study the application of our results on 3 different experimental systems: ultra-cold atoms with long range interactions on optical lattices in both square and honeycomb lattice in section VII, adatom adsorption on different substrates such as possible reentrant supersolids in the second layer of ${}^4\text{He}$ adsorbed on graphite and Hydrogen adsorbed on Krypton-preplated graphite in honeycomb lattice in section VIII, possible cooper pair supersolid in high temperature superconductor $\text{La}_{2-x}\text{Ba}_x\text{CuO}_4$ in square lattice in section IX. finally, we reach conclusions in section X. In the appendix, we review the boson-vortex duality at integer filling $f = n$ in which I will stress the role of the dual gauge field and its connection to the more general case of $f = p/q$ developed in^{5,10} and the main text of this

paper.

II. MAGNETIC SPACE GROUP, EFFECTIVE ACTION AND ORDER PARAMETERS IN THE DUAL VORTEX PICTURE.

In this section, we will extend the DVM in⁵ to study the EBHM Eqn.1 in honeycomb lattice at and *slightly away* from $q = 2$. Honeycomb lattice (solid line in Fig.1) is not a Bravais lattice, so may show some different properties than a square lattice. The dual lattice of the honeycomb lattice is a triangular lattice (dashed line in Fig.1). Two basis vectors of a primitive unit cell of the triangular lattice can be chosen as $\vec{a}_1 = \hat{x}, \vec{a}_2 = -\frac{1}{2}\hat{x} + \frac{\sqrt{3}}{2}\hat{y}, \vec{a}_d = \vec{a}_1 + \vec{a}_2$ as shown in Fig.1. The reciprocal lattice of a triangular is also a triangular lattice and spanned by two basis vectors $\vec{k} = k_1\vec{b}_1 + k_2\vec{b}_2$ with $\vec{b}_1 = \hat{x} + \frac{\hat{y}}{\sqrt{3}}, \vec{b}_2 = \frac{2}{\sqrt{3}}\hat{y}$ satisfying $\vec{b}_i \cdot \vec{a}_j = \delta_{ij}$. The point group of a triangular lattice is $C_{6v} \sim D_6$ which contains 12 elements. The two generators can be chosen as $C_6 = R_{\pi/3}, I_1$. The space group also includes the two translation operators T_1 and T_2 along \vec{a}_1 and \vec{a}_2 directions respectively. The 3 translation operators T_1, T_2, T_d , the rotation operator $R_{\pi/3}$, the 3 reflection operators I_1, I_2, I_d , the two rotation operators around the direct lattice points A and B : $R_{2\pi/3}^A, R_{2\pi/3}^B$ of the MSG are worked out in the following.

In the Landau gauge $\vec{A} = (0, Hx)$, the mean field Hamiltonian for the vortices hopping in a triangular lattice in the presence of f flux quanta per triangle in the tight-binding limit is⁵ :

$$\begin{aligned} H_{0v} = & -t \sum_{\vec{x}} [|\vec{x} + \vec{a}_1\rangle \langle \vec{x}| + h.c. \\ & + |\vec{x} + \vec{a}_2\rangle \langle \vec{x}| + h.c. \\ & + |\vec{x} + \vec{a}_d\rangle \langle \vec{x}| + h.c.] \quad (3) \end{aligned}$$

where $\vec{x} = a_1\vec{a}_1 + a_2\vec{a}_2$ denotes lattice points of the triangular lattice. Note that the total vortex Hamiltonian $H_v = H_{0v} + V$ where V is the interaction between vortices. Because V does not contain any Aharonov-Bohm (AB) phase factor from the non-trivial A_μ background, so the magnetic space group is completely determined by the vortex kinetic term H_{0v} . V always commutes with the generators of the MSG given by Eqns. 4,5,10. So when constructing the representation of the MSG, we can ignore the V term without losing any generality.

The T_1, T_2, T_d and the rotation operator $R_{\pi/3}$ of the PSG are worked out in⁵. Here we listed them in slightly

different notations:

$$\begin{aligned}
T_1 &= \sum_{\vec{x}} |\vec{x} + \vec{a}_1 \rangle e^{i2\pi 2f a_2} \langle \vec{x}| \\
T_2 &= \sum_{\vec{x}} |\vec{x} + \vec{a}_2 \rangle \langle \vec{x}| \\
T_d &= \sum_{\vec{x}} |\vec{x} + \vec{a}_d \rangle e^{i2\pi 2f(a_2+1/2)} \langle \vec{x}| \\
R_{\pi/3} &= \sum_{\vec{x}} e^{i2\pi f(a_1^2 - 2a_1 a_2)} |a_1 - a_2, a_1 \rangle \langle a_1, a_2| \quad (4)
\end{aligned}$$

It can be shown that they all commute with H . However, they do not commute with each other $T_1 T_2 = \omega T_d, T_1 T_2 = \omega^2 T_2 T_1$.

After performing some algebras, we found three of the 6 reflection operators in the point group C_{6v} :

$$\begin{aligned}
I_1 &= K \sum_{\vec{x}} e^{-i2\pi f a_2^2} |a_1 - a_2, -a_2 \rangle \langle a_1, a_2| \\
I_2 &= K \sum_{\vec{x}} e^{-i2\pi f a_1^2} |-a_1, a_2 - a_1 \rangle \langle a_1, a_2| \\
I_d &= K \sum_{\vec{x}} e^{-i2\pi f 2a_1 a_2} |a_2, a_1 \rangle \langle a_1, a_2| \quad (5)
\end{aligned}$$

where K is the complex conjugate operator which make I_1, I_2, I_3 non-unitary operators. Note that in contrast to the reflection operators in square lattice, the phase factors in Eqn.5 are crucial to ensure they commute with the Hamiltonian Eqn.3.

The eigenvalue equation $H\psi(\vec{k}) = E(\vec{k})\psi(\vec{k})$ leads to the Harper's equation in the triangle lattice:

$$\begin{aligned}
&(e^{-ik_1} + e^{-i(k_1+k_2+2\pi f(2l-1))})\psi_{l-1}(k_1, k_2) \\
&+ (e^{ik_1} + e^{i(k_1+k_2+2\pi f(2l-1))})\psi_{l+1}(k_1, k_2) \\
&+ 2\cos(-k_2 + 2\pi fl)\psi_l(k_1, k_2) = E(\vec{k})\psi_l(k_1, k_2) \quad (6)
\end{aligned}$$

where $l = 0, 1, \dots, q-1$.

In the following, we focus on $q = 2$ case where there is only *one* band $E(\vec{k}) = -2t(\cos k_1 + \cos k_2 - \cos(k_1 + k_2))$. Obviously, $E(k_1, k_2) = E(-k_1, -k_2) = E(k_2, k_1)$. There are *two* minima at $\vec{k}_{\pm} = \pm(\pi/3, \pi/3)$. Let's label the two eigenmodes at the two minima as ψ_{\pm} . By using the expressions of the rotation and reflection operators in Eqns. 4, 5, we find the two fields transform as:

$$\begin{aligned}
T_1, T_2 : \psi_{\pm} &\rightarrow e^{\mp i\pi/3} \psi_{\pm}; \quad T_d : \psi_{\pm} \rightarrow -e^{\mp i2\pi/3} \psi_{\pm} \\
R_{\pi/3} : \psi_{\pm} &\rightarrow \psi_{\mp}; \quad I_{\alpha} : \psi_{\pm} \rightarrow \psi_{\mp}^*, \quad \alpha = 1, 2, d \quad (7)
\end{aligned}$$

where the transformations under $T_{\alpha}, R_{\pi/3}$ were already derived in⁵. Note that $R_{\pi/3}$ plays the same role as the Z_2 exchange symmetry between ψ_+ and ψ_- .

The quadratic terms of the effective action is simply the scalar electrodynamics as in the square lattice case:

$$\mathcal{L}_0 = \sum_{\alpha=\pm} |(\partial_{\mu} - iA_{\mu})\psi_{\alpha}|^2 + r|\psi_{\alpha}|^2 + \frac{1}{4}F_{\mu\nu}^2 \quad (8)$$

where $F_{\mu\nu} = \frac{1}{2}\epsilon_{\mu\nu\lambda}\partial_{\nu}A_{\lambda}$ is the strength of the non-compact gauge field A_{μ} .

It is easy to show that there are only 2 independent quartic invariants under the above transformations:

$$\Lambda_1 = |\psi_+|^4 + |\psi_-|^4, \quad \Lambda_2 = |\psi_+|^2|\psi_-|^2 \quad (9)$$

The direct honeycomb lattice is a non-Bravais lattice which contains two lattice points A and B per direct unit cell, it is useful to work out the rotation operators around the direct lattice points A and B which contain new symmetries not included in the rotation operator around a dual triangular lattice point $R_{\pi/3}$:

$$\begin{aligned}
R_{2\pi/3}^A &= \sum_{\vec{x}} e^{i2\pi f(a_2^2 - 2a_1 a_2 - 2a_1 - 2a_2)} \\
&|-a_2 + 1, a_1 - a_2 \rangle \langle a_1, a_2| \\
R_{2\pi/3}^B &= \sum_{\vec{x}} e^{i2\pi f((a_2-1)^2 - 2a_1 a_2 + 2a_1)} \\
&|-a_2 + 1, a_1 - a_2 + 1 \rangle \langle a_1, a_2| \quad (10)
\end{aligned}$$

They act on the two vortex fields ψ_{\pm} as:

$$R_{2\pi/3}^A : \psi_{\pm} \rightarrow e^{\mp i\pi/3} \psi_{\pm}; \quad R_{2\pi/3}^B : \psi_{\pm} \rightarrow e^{\pm i\pi/3} \psi_{\pm} \quad (11)$$

It is ease to see the two operators Λ_1, Λ_2 in Eqn.9 are also invariant under Eqn.11. Finally we reach the most general quartic term invariant under all the above transformations in Eqns.7, 11:

$$\mathcal{L}_4 = \gamma_0(|\psi_+|^2 + |\psi_-|^2)^2 - \gamma_1(|\psi_+|^2 - |\psi_-|^2)^2 \quad (12)$$

In the square lattice, In Landau gauge, a unitary transformation to the permutative representation is needed to reach Eqn.12. Here in the gauge chosen in Eqn.3, ψ_{\pm} are automatically in the permutative representation. An important and subtle point is how to construct boson density order parameters to characterize the symmetry breaking patterns in the direct lattice in terms of the dual vortex fields in the dual lattice. In⁵, the density order parameter was constructed to be the most general gauge invariant and *bilinear* combinations of the vortex fields ψ_l . Then it was evaluated at the direct lattice points, links and dual lattice points to represent boson density, kinetic energy and amplitude of the ring exchanges respectively. The dual lattice of a square lattice is still a square lattice with the same lattice constant. The link points of a square lattice also form a square lattice with lattice constant $\sqrt{2}$. Putting the direct, dual and link lattices together forms a square lattice with lattice constant 1/2. Although like a square lattice, the honeycomb lattice is also a bi-partisan lattice consisting of two interpenetrating triangular sublattices A and B , its dual lattice is a triangular lattice which is a frustrated one (Fig.1), its link points form a Kagome lattice. Putting the three lattices together forms a very complicated lattice. So the density wave order parameters in the honeycomb lattice may not be evaluated in the three lattices. Indeed,

when trying to identify the density operators in the insulating state, we find the density operators proposed in⁵ does not apply anymore in the honeycomb lattice. In the following, by studying how gauge invariant bilinear vortex fields transform under the complete PSG, we can identify both the boson density and boson kinetic energy operators in the direct lattice. We need evaluate these quantities *only* at dual lattice points to characterize the CDW and VBS orders in the direct lattice. Let's look at the *generalized* density order operators which characterize the symmetry breaking patterns in the insulating states. In the low energy limit, the vortex field is:

$$\psi(\vec{x}) = e^{-i\vec{k}_+ \cdot \vec{x}} \psi_+(\vec{x}) + e^{-i\vec{k}_- \cdot \vec{x}} \psi_-(\vec{x}) \quad (13)$$

Intuitively, the generalized density operator $\rho(\vec{x}) = \psi^\dagger(\vec{x})\psi(\vec{x})$ can be written as:

$$\rho(\vec{x}) = \psi_+^\dagger \psi_+ + \psi_-^\dagger \psi_- + e^{i\vec{Q} \cdot \vec{x}} \psi_+^\dagger \psi_- + e^{-i\vec{Q} \cdot \vec{x}} \psi_-^\dagger \psi_+ \quad (14)$$

where $\vec{Q} = 2\pi/3(1,1)$.

When taking continuum limit on the dual lattice, we take one site per dual unit cell which contains two direct lattice sites A and B (Fig. 1). So Eqn.14 should contain both the information on the boson densities on sites A and B and the boson kinetic energy on the link between A and B (or XY exchange energy $< S_A^+ S_B^- + h.c. >$ in the spin language). The single boson Green function hopping on the direct lattice is related to the gauge-invariant single vortex Green function on the dual lattice in a highly non-local way²¹. Fortunately, the two boson quantities such as the density and the kinetic energy may have simple local expressions in terms of the dual vortex fields. By studying how the operators in Eqn. 14 transform under 7 and 11, in the scaling limit, we can identify these quantities as (up to a unknown prefactor)²² :

$$\begin{aligned} \rho_A &= \psi_+^\dagger \psi_+, & \rho_B &= \psi_-^\dagger \psi_- \\ K_{AB} &= e^{i\vec{Q} \cdot \vec{x}} \psi_+^\dagger \psi_- + e^{-i\vec{Q} \cdot \vec{x}} \psi_-^\dagger \psi_+ \end{aligned} \quad (15)$$

where \vec{x} stands for dual lattice points *only*.

Moving *slightly* away from half filling $f = 1/2$ corresponds to adding a small *mean* dual magnetic field $H \sim \delta f = f - 1/2$ in the action. It can be shown that *inside the SF phase*, the most general action invariant under all the MSG transformations upto quartic terms is :

$$\begin{aligned} \mathcal{L}_{SF} &= \sum_{\alpha=a/b} |(\partial_\mu - iA_\mu)\psi_\alpha|^2 + r|\psi_\alpha|^2 \\ &+ \frac{1}{4e^2} (\epsilon_{\mu\nu\lambda} \partial_\nu A_\lambda - 2\pi\delta f \delta_{\mu\tau})^2 + \mathcal{L}_4 \end{aligned} \quad (16)$$

where A_μ is a non-compact $U(1)$ gauge field. Upto the quartic level, with correspondingly defined $\psi_{a/b}$ in a square lattice, Eqn.16 is *the same* as that in the square lattice derived in⁵. Because Eqn.16 is a long wavelength effective action, the relations between the phenomenological parameters in Eqn.16 and the microscopic parameters in Eqn.1 are not known. Fortunately, we are still able

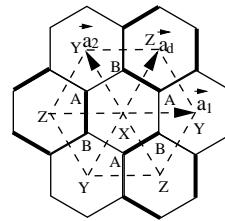


FIG. 1: (a) Bosons at filling factor f are hopping on a honeycomb lattice (solid line) which has two sublattices A and B . Vortices are hopping on its dual lattice which is a triangular lattice (dashed line) which has three sublattices X, Y, Z . In the easy-plane limit shown in Fig.2c, one of the three VBS states¹⁶ on the honeycomb lattice is shown by the thick bonds in the figure. The other two VBS can be obtained by $R_{2\pi/3}^A$ or $R_{2\pi/3}^B$.

to classify some phases and phase transitions and make some concrete predictions from Eqn.16 without knowing these relations. In the following, we assume $r < 0$ in Eqn.8, so the system is in insulating states. We will discuss the Ising limit and the easy-plane limit respectively.

III. ISING LIMIT

If $\gamma_1 > 0$, the system is in the Ising limit, the mean field solution is $\psi_a = 1, \psi_b = 0$ or vice versa. The system is in the CDW order. We can see how ρ_A, ρ_B transform under Eqns. 7 and 11:

$$T_\alpha, R_{2\pi/3}^{A/B} : \rho_{A/B} \rightarrow \rho_{A/B}; \quad R_{\pi/3}, I_\alpha : \rho_A \leftrightarrow \rho_B \quad (17)$$

These transformations confirm that ρ_A and ρ_B indeed can be identified as the boson density operators at direct sublattices A and B . In this section, we discuss at and away from half filling respectively.

A. SF to CDW transition at half filling $\delta f = 0$.

If $r < 0$, the system is in the CDW order which could take checkboard (π, π) order or a stripe order¹⁷. Eqn.16 is an expansion around the uniform saddle point $\langle \nabla \times \vec{A} \rangle = f = 1/2$ which holds in the SF and the VBS (to be discussed in section 4), so it breaks down in the CDW side. So it can not be used to study the SF to the CDW transition.

In the CDW state where $r < 0$, a different saddle point where $\langle \nabla \times \vec{A}^a \rangle = 1 - \alpha$ for sublattice A and $\langle \nabla \times \vec{A}^b \rangle = \alpha$ for sublattice B with $\alpha < 1/2$ should be used. It is easy to see that there is only one vortex minimum ψ_b in the staggered dual magnetic field at $\delta f = 0$, the effective action *inside* the CDW state is:

$$\begin{aligned} \mathcal{L}_{C-CDW} &= |(\partial_\mu - iA_\mu^b)\psi_b|^2 + \tilde{r}|\psi_b|^2 + \tilde{u}|\psi_b|^4 + \dots \\ &+ \frac{1}{4\tilde{e}^2} (\epsilon_{\mu\nu\lambda} \partial_\nu A_\lambda^b)^2 \end{aligned} \quad (18)$$

where $\tilde{r} < 0$, so the system is in the CDW state where $\langle \psi_b \rangle \neq 0$. Eqn.18 is essentially the same as Eqn.A2 in $q = 1$ case. Note that because $\langle \psi_a \rangle \neq 0$, the gauge field \vec{A}^a is always massive, so it does not appear in Eqn.18. As explained in the appendix, this indicates the density fluctuations in sublattice A is suppressed, so can be taken as fixed.

Due to the change of the saddle point structures, the transition from the SF to the CDW driven by the horizontal axis (quantum fluctuation r) in Fig.2b is a *strong* first order transition. If we assumed that Eqn.16 at $\delta f = 0$ in the Ising limit could be used to describe this first order transition, then the CDW side could be described by $\langle \psi_a \rangle \neq 0, \langle \psi_b \rangle = 0$ or vice versa⁵⁰, but no phases with $\langle \psi_a \rangle \neq 0, \langle \psi_b \rangle \neq 0$. However, as shown in Eqn.18, in the CDW side, $\langle \psi_a \rangle \neq 0, \langle \psi_b \rangle \neq 0$, so both gauge fields \vec{A}^a and \vec{A}^b are massive, the density fluctuations in both sublattice A and B are suppressed, so both can be taken as fixed. This fact is due to the change of saddle point structure across the SF to the CDW transition. So we conclude that due to this change of saddle point structure of the dual gauge fields across the SF to the CDW, Eqn.16 at $\delta f = 0$ in the Ising limit can not be used to describe this first order transition. However, it does give a qualitative indication of this strong first order transition. This is expected, because in a strong first order transition, two separate dual actions Eqn.16 in the SF side and Eqn.18 are needed to describe the two sides separately. Note that in the direct picture, the SF breaks the $U(1)$ symmetry, the CDW breaks the lattice symmetry, so the two sides break two completely different symmetries, it can only be first order.

B. Charge Density Wave (CDW) supersolid away from half filling $\delta f \neq 0$.

Now we look at the effects of the in-commensurability $\delta f = f - 1/2$ in Eqn.18. In the SF side where $r > 0$, it is known the SF is stable against the change of the chemical potential (or adding bosons). In the CDW side where $\tilde{r} < 0$, moving *slightly* away from half filling $f = 1/2$ corresponds to adding a small *mean* dual magnetic field $H \sim \delta f = f - 1/2$ in Eqn.18:

$$\begin{aligned} \mathcal{L}_{IC-CDW} = & |(\partial_\mu - iA_\mu^b)\psi_b|^2 + \tilde{r}|\psi_b|^2 + \tilde{u}|\psi_b|^4 + \dots \\ & + \frac{1}{4\tilde{e}^2}(\epsilon_{\mu\nu\lambda}\partial_\nu A_\lambda^b - 2\pi\delta f\delta_{\mu\tau})^2 \end{aligned} \quad (19)$$

where the vortices in the phase winding of ψ_b should be interpreted as the the boson number¹⁸. Note that because $\langle \psi_a \rangle \neq 0$ and remains non-zero in the presence of δf , the gauge field \vec{A}^a is always massive and remains massive in the presence of δf , so it still does not appear in Eqn.18. This indicates the density fluctuations in sublattice A remains suppressed, so can be taken as fixed in the presence of δf .

Eqn.19 is essentially the same as Eqn.A4 which has the structure identical to the conventional $q = 1$ component

Ginzburg-Landau model for type-II " superconductors " in a "magnetic" field. It was shown in¹⁹ that for type II superconductors, the gauge field fluctuations will render the vortex fluid phase intruding at H_{c1} between the Messiner and the mixed phase (see Fig. 2a). For parameters appropriate to the cuprate superconductors, this intrusion occurs over too narrow an interval of H to be observed in experiments. In the present boson problem with the nearest neighbor interaction $V_1 > 0$ in Eqn.1 which stabilizes the (π, π) CDW state at $f = 1/2$, along the dashed line driven by the vertical axis (chemical potential μ) in Fig.2b, this corresponds to a CDW supersolid (CDW-SS) state intruding between the commensurate CDW state at $f = 1/2$ and the in-commensurate CDW state at $1/2 + \delta f$ which could be stabilized by further neighbor interactions in Eqn.1. The first transition is in the $z = 2, \nu = 1/2, \eta = 0$ universality class first discussed in¹, while the second is a 1st order transition. We expect the intruding window at our $q = 2$ system is much wider than that of the $q = 1$ system. In the CDW states, $\langle \psi_b \rangle \neq 0$, so the dual gauge field \vec{A}_μ^b in Eqn.19 is massive. In the CDW-SS state, $\langle \psi_b \rangle = 0$, there is the gapless superfluid mode represented by the dual gauge field A_μ^b . The CDW-SS has the same (π, π) diagonal order as the C-CDW. The identified universality class of the CDW to the CDW-SS transition has many physical implications. For example, near the C-CDW to the CDW-SS transition, the superfluid density should scale as $\rho_s \sim |\rho - 1/2|^{(d+z-2)\nu} = |\rho - 1/2| = \delta f$ with a logarithmic correction. The logarithmic correction will be calculated in a future publication . There must be a transition from the CDW-SS to the SF inside the window driven by the quantum fluctuation r in the Fig.2b. The universality class of this transition is likely to be first order and will be investigated further in a future publication . Combining the results in III-A and III-B leads to the global phase diagram Fig.2b in the Ising limit²⁴.

IV. EASY-PLANE LIMIT.

If $\gamma_1 < 0$, the system is in the easy-plane limit, the mean field solution is $\psi_a = e^{i\theta_a}, \psi_b = e^{i\theta_b}$, then $\rho_A = \rho_B = 1$, so the two sublattices remain equivalent. This limit could be reached by possible ring exchange interactions in Eqn.1. In the following, we discuss at and away from half filling respectively.

A. SF to VBS transition at half filling $\delta f = 0$.

Because the two sublattices remain equivalent, the uniform saddle point $\langle \nabla \times \vec{A} \rangle = f = 1/2$ holds in both the SF and the VBS. The system has a VBS order with the kinetic energy order parameter $K_{AB} = \cos(\vec{Q} \cdot \vec{x} + \theta_-)$ where $\theta_- = \theta_a - \theta_b$. Let's look at how the kinetic energy

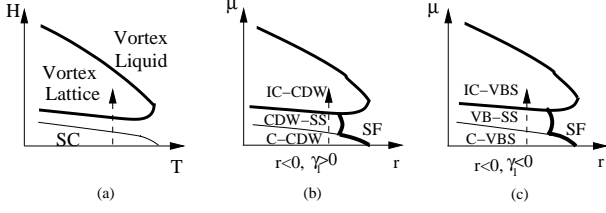


FIG. 2: (a) The phase diagram *slightly away* from $f = 1$ described by Eqn.A4 in the appendix is the same as type-II superconductors in an external magnetic field H where there should be a vortex liquid state intruding between the Messiner state and the vortex lattice state. But the intruding regime is too narrow to be seen in type-II superconductors¹⁹. (b) and (c) are the zero temperature global phase diagrams of the chemical potential μ versus r in Eqn.16 in the honeycomb lattice. (b) The Ising limit $\gamma_1 > 0$ discussed in section III. There is a CDW supersolid (CDW-SS) state intruding between the commensurate CDW (C-CDW) state at $f = 1/2$ and the in-commensurate CDW (IC-CDW) state at $1/2 + \delta f$. The CDW-SS has the same lattice symmetry breaking as the C-CDW. (c) The Easy-Plane limit $\gamma_1 < 0$ discussed in section IV. There is a Valence Bond Supersolid (VB-SS) state intruding between the commensurate VBS (C-VBS) state at $f = 1/2$ and the in-commensurate VBS (IC-VBS) state at $1/2 + \delta f$. The VB-SS has the same lattice symmetry breaking as the C-VBS. The thin (thick) line is the 2nd (1st) order transition. The 1st order transition in the Ising (Easy-plane) limit is *strong* (*weak*) one. (b) and (c) are drawn only above half filling. $\mu \rightarrow -\mu$ corresponds to below half filling.

K transform:

$$\begin{aligned} T_\alpha &: K \rightarrow \cos(\vec{Q} \cdot (\vec{x} - \vec{a}_\alpha) + \theta) \\ R_{\pi/3} &: K \rightarrow \cos(\vec{Q} \cdot \vec{x} - \theta); \quad I_\alpha : K \rightarrow K \\ R_{2\pi/3}^{A/B} &: K \rightarrow \cos(\vec{Q} \cdot \vec{x} + \theta \mp 2\pi/3) \end{aligned} \quad (20)$$

Note that K transforms differently under $R_{\pi/3}$ and I_α , because the latter are anti-unitary operators. These transformations confirm that K indeed can be identified as the boson kinetic energy or the XY exchange energy operators at the direct lattice.

Upto the quartic order, the relative phase between ψ_+ and ψ_- is undetermined. Higher order terms are needed to determine the relative phase. It is clear to see there are only 3 sixth order invariants:

$$\begin{aligned} C_1 &= |\psi_+|^6 + |\psi_-|^6 \\ C_2 &= (|\psi_+|^2 + |\psi_-|^2)|\psi_+|^2|\psi_-|^2 \\ C_3 &= \lambda[(\psi_+^* \psi_-)^3 + (\psi_-^* \psi_+)^3] = \lambda \cos 3\theta \end{aligned} \quad (21)$$

where $\theta = \theta_+ - \theta_-$. Especially C_3 is invariant under $R_{2\pi/3}^{A/B}$. Obviously, only the last term C_3 can fix the relative phase. This term corresponds to the 3-monopole operator in the spin language.

If $\lambda > 0$, $\theta = (2n + 1)\pi/3 = \pi/3, \pi, -\pi/3$. The kinetic energy $K = 1, -2, 1$ takes only two values, one strong bond and two weak bonds, their ratio is 2. The dual

triangular lattice can be divided into three sublattices X, Y, Z where $x_1 + x_2 = 0, 1, 2 \pmod 3$, hence $\vec{Q} \cdot \vec{x} = 0, 2\pi/3, -2\pi/3$ respectively (Fig.1). If we evaluate K at X, Y, Z , we find $K_X = \cos \theta, K_Y = \cos(\theta + 2\pi/3), K_Z = \cos(\theta - 2\pi/3)$. If we know one bond in one dual unit cell, say, labeled by X , then by the translation, we can get all the other bonds in sublattices Y and Z with the same orientation. The two bonds on the other two orientations can be reached by rotations listed in Eqn. 20. By this way, we can get all the bonds in the whole direct lattice. So the system is in the Valence Bond Solid (VBS) state, one VBS is shown in Fig.1.

If $\lambda < 0$, $\theta = 2n\pi/3 = 0, 2\pi/3, -2\pi/3$. The kinetic energy $K = 2, -1, -1$ takes also only two values, one strong bond and two weak bonds, their ratio is also 2. This case is essentially the same as $\lambda > 0$. Because the sign of the kinetic term can be changed in a bi-partisan lattice by changing the sign of b_i in one of the two sublattices in Eqn.1 (or can be changed by changing the sign of S_i^x, S_i^y in one of the two sublattices, but keeping S_i^z untouched in Eqn.2), but the product of the sign around a hexagon is fixed. The two cases have the same sign product, so can be transformed to each other by the transformation. This can also be understood by observing that C_3 in Eqn.21 behaves like a hopping term in 3 power, so its sign can be changed by the transformation. This is in sharp contrast to the square lattice to be discussed in section V where one sign leads to a columnar dimer, the other leads to a plaquette pattern.

B. Valence Bond Supersolid away from half filling $\delta f \neq 0$.

Now we look at the effects of the in-commensurability $\delta f = f - 1/2$ in Eqn.16. Again, the SF side where $r > 0$ is stable against the change of the chemical potential. In the VBS side where $r < 0$, slightly away from the half-filling, Eqn.16 becomes:

$$\begin{aligned} \mathcal{L}_{VBS} &= \left(\frac{1}{2}\partial_\mu \theta_+ - A_\mu\right)^2 + \frac{1}{4e^2}(\epsilon_{\mu\nu\lambda} \partial_\nu A_\lambda - 2\pi\delta f \delta_{\mu\tau})^2 + \dots \\ &+ \left(\frac{1}{2}\partial_\mu \theta_-\right)^2 + 2\lambda \cos 3\theta_- \end{aligned} \quad (22)$$

where $\theta_\pm = \theta_a \pm \theta_b$.

Obviously, the θ_- sector is massive (namely, θ_a and θ_b are *locked* together) and can be integrated out. Assuming $\lambda > 0$, then $\theta_- = \pi$. Setting $\psi_+ = e^{i\theta_+} \sim \psi_a \sim -\psi_b$ in Eqn.16 leads to Eqn.19 with $\tilde{u} = 2\gamma_0$, so the discussions on Ising limit case following Eqn.19 also apply. In the present boson problem with possible ring exchange interactions in Eqn.1 which stabilizes the VBS state at $f = 1/2$, along the dashed line driven by the vertical axis (chemical potential μ) in Fig.2c, this corresponds to a VBS supersolid (VB-SS) state intruding between the commensurate VBS (C-VBS) state at $f = 1/2$ and the in-commensurate VBS (IC-VBS) state at $1/2 + \delta f$ as shown in Fig.2c. In the C-VBS state described in the

subsection A, $\langle \psi_a \rangle = -\langle \psi_b \rangle \neq 0$, $\langle \psi_a^\dagger \psi_a \rangle = \langle \psi_b^\dagger \psi_b \rangle = -\langle \psi_a^\dagger \psi_b \rangle \neq 0$, the gauge field A_μ is massive due to the Higgs mechanism. In the VB-SS state, $\langle \psi_a \rangle = \langle \psi_b \rangle = 0$, but $\langle \psi_a^\dagger \psi_a \rangle = \langle \psi_b^\dagger \psi_b \rangle = -\langle \psi_a^\dagger \psi_b \rangle \neq 0$, so there is a VBS order characterized by the order parameter $K_{AB} = \cos(\vec{Q} \cdot \vec{x} + \theta_-)$ which is the same as the C-VBS, while the gauge field A_μ is massless which stands for the gapless superfluid mode inside the VB-SS. So this VB-SS has both the VBS order and the superfluid order which justifies its name. *So in this VB-SS, the density fluctuation on each site is very large signaling its superfluid nature, while the VBS order is fixed signaling its VBS nature.* In this IC-VBS state, δf valence bonds shown in Fig.1 is slightly stronger than the others, these δf slightly stronger bonds also form a dilute lattice on top of the underlying C-VBS lattice. Again, the first transition from the C-VBS to the VB-SS is in the $z = 2, \nu = 1/2, \eta = 0$ universality class, while the second from the VB-SS to the IC-VBS is 1st order. Near the C-VBS to the VB-SS transition, the superfluid density should scale as $\rho_s \sim |\rho - 1/2|^{(d+z-2)\nu} = |\rho - 1/2| = \delta f$ with logarithmic corrections. The nature of the transition from the VB-SS to the SF where $\langle \psi_a \rangle = \langle \psi_b \rangle = 0$ and $\langle \psi_a^\dagger \psi_b \rangle = 0$ inside the window driven by the quantum fluctuation r in the Fig.2c is likely to be weakly first order and will be studied further in a future publication. Combining (4a) and (4b) leads to the global phase diagram in Fig.2c.

V. SQUARE LATTICE.

As said below Eqn.16, with correspondingly defined $\psi_{a/b}$ in a square lattice, upto the quartic level, Eqn.16 is the same as that in the square lattice derived in⁵.

A. Ising limit

So the phase diagram in the Ising limit Fig.3b remains the same as Fig.2b. The SF to the C-CDW transition at $\delta f = 0$ along the horizontal axis is a *strong* first order one. Away from the half filling, along the dashed line in Fig.3b, the IC-CDW can be stabilized only by very long range interactions in Eqn.1, if it is not stable, then Fig.3b reduces to Fig. 4b (which is the Fig.14 in¹⁴).

B. Easy-plane limit

In the Easy-plane limit, as shown in⁵, the lowest order term coupling the two phases $\theta_{a/b}$ is $C_{sq} = \lambda \cos 4\theta$, so the C_3 term in Eqn.22 need to be replaced by C_{sq} . If λ is positive (negative), the VBS is Columnar dimer (plaquette) pattern⁵.

By using duality analysis and QMC simulation, the author in²⁵ suggested that in the easy plane limit, the $q = 2$

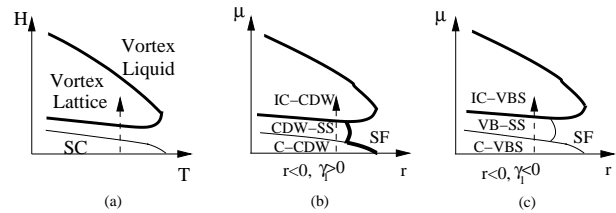


FIG. 3: Phase diagram in square lattice. (a) is identical to 2a and presented here just for completeness. (b) is similar to Fig.2b on the honeycomb lattice in the Ising limit. In the easy plane limit (c), there is a possible 2nd order transition between the SF and the C-VBS through a so called deconfined quantum critical point. However, this has been disputed in²⁶.

component scalar electrodynamics Eqn.16 at $\delta f = 0$ along the horizontal axis is a second order transition through a so called "de-confined QCP". If this is indeed the case, then $C_{sq} = \lambda \cos 4\theta$ is irrelevant, there is a possible 2nd order transition between the SF and the C-VBS through a so called deconfined quantum critical point as shown in Fig.3c. Away from the half filling, along the dashed line in Fig.3c, the phase transitions are the same as those in the honeycomb lattice Fig. 2c. The transition from the VB-SS to the SF where $\langle \psi_a \rangle = \langle \psi_b \rangle = 0$ and $\langle \psi_a^\dagger \psi_b \rangle = 0$ inside the window driven by the quantum fluctuation r in the Fig.3c is also through line of deconfined quantum critical points. Recently, some connections are made between the correlation functions (which lead to transport properties such as conductivity) near the deconfined quantum critical point in Fig.3c and those in $\mathcal{N} = 8$ supersymmetric $SU(N)$ Yang-Mills gauge theory in the large N limit at $d = 2$ ⁴⁹. These correlation functions were calculated through $AdS_4 \times S^7/CFT_3$ connection⁴⁹. The particle-vortex self-duality in Fig.3c and corresponding electromagnetic self-duality in $AdS_4 \times S^7/CFT_3$ put strong constraints on correlation functions in the two models respectively.

However, recently, by using QMC simulations at much larger systems, the authors in²⁶ pointed out that the QMC study in²⁵ violates the hyperscaling and concluded that there is no such deconfined QCP, so the transition from SF to the VBS driven by the horizontal axis (quantum fluctuation r) is a *weak* first order one. If this is indeed the case, the phase diagram in the easy-plane limit remains the same as in a honeycomb lattice Fig.2c.

VI. IMPLICATION ON QUANTUM MONTE-CARLO (QMC) SIMULATIONS.

The EBHM Eqn.1 of the hard core bosons on square lattice with V_1 and V_2 interactions was studied by the QMC simulations in¹⁴, the authors found a stable striped $(\pi, 0)$ and $(0, \pi)$ SS (Fig.4). A stable (π, π) SS can only be realized in the soft core boson case¹⁵. But the

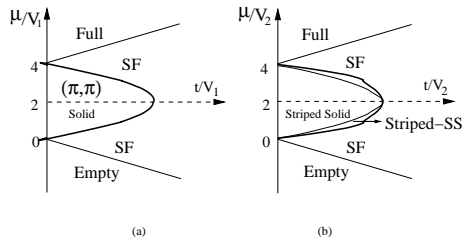


FIG. 4: Phase diagrams of the EBHM Eqn.1 in the hard core limit $U = \infty$ achieved from the QMC in¹⁴: (a) with the nearest neighbor interaction $V_1 > 0$, the CDW ordering wavevector is (π, π) . The corresponding (π, π) supersolid is unstable against the phase separation. However, it becomes stable in the soft core limit¹⁵ (b) $V_1 = 0$, but next nearest neighbor interaction $V_2 > 0$, the CDW ordering wavevector is $(\pi, 0)$ or $(0, \pi)$ which is called stripe phase. The corresponding stripe supersolid is stable even in the hard core limit. So there is a narrow window of stripe SS intervening between the stripe solid and the SF. The universality class of the stripe solid to the stripe SS in (b) was not studied in¹⁴. The thin (thick) line is a 2nd (1st) order transition.

nature of the CDW to supersolid transition has never been addressed. Our results in the Fig.3 show that the CDW to the SS transition must be in the same universality class of Mott to superfluid transition with exact exponents $z = 2, \nu = 1/2, \eta = 0$ with a logarithmic correction. It is important to (1) confirm this prediction by finite size scaling through the QMC simulations in square lattice for $(0, \pi)$ and $(\pi, 0)$ supersolid in both hard core and soft core case in the Fig.4 and (π, π) supersolid in the soft core case only (2) do similar things in honeycomb lattice to confirm Fig.1. Some of our results in Fig.3 are indeed confirmed in very recent QMC simulations on soft core bosons in honeycomb lattice²⁰. (3) To Eqn.1 with $U = \infty, V_1 > 0$, adding a ring exchange term $-K_s \sum_{ijkl} (b_i^\dagger b_j b_k^\dagger b_l + h.c.)$ where i, j, k, l label 4 corners of a square in the square lattice and $-K_h \sum_{ijklmn} (b_i^\dagger b_j b_k^\dagger b_l b_m^\dagger b_n + h.c.)$ where i, j, k, l, m, n label 6 corners of a hexagon in the honeycomb lattice to stabilize the C-VBS state *at half filling* (Note that if $K_s, K_h > 0$, the QMC are free of sign problems), then confirm the prediction on C-VBS to VB-SS transition in Fig.2c and Fig.3c. We expect that the VB-SS phase should be stable against a phase separation in both hard and soft core cases. The second transition (CDW-SS to IC-CDW in Fig.2b and Fig.3b and the VB-SS to IC-VBS in Fig. 2c and Fig.3c) is hard to be tested in QMC, because some very long range interactions are needed to stabilize the IC-CDW or the IC-VBS state. They are first order transition anyway.

In fact, one of the predictions in this paper on the scaling of the superfluid density $\rho_s \sim |\rho - 1/2|$ was already found in the striped $(\pi, 0)$ solid to striped supersolid transition by QMC in Sec.V-B of Ref.¹⁴. As shown in section III-B, there should be a logarithmic correction to the scaling of ρ_s , it remains a challenge to detect the loga-

rithmic correction by a high precision QMC. Of course, the superfluid density is anisotropic $\rho_s^x > \rho_s^y$ in the $(\pi, 0)$ supersolid, but they scale in the same way with different coefficients¹⁴. Although the authors in¹⁴ suggested it is a 2nd order transition, they did not address the universality class of the transition.

In the following three sections, I will discuss the applications of the results achieved in the previous sections on 3 different experimental systems.

VII. ULTRA-COLD ATOM ON SQUARE AND HONEYCOMB OPTICAL LATTICES

Recently, Bose-Einstein condensation (BEC) was realized in ultra-cold atomic gases (for a review , see²⁸). Superfluid to Mott insulator transition was also observed in optical lattices of ultra-cold alkali atoms²⁷. Atomic physicists are constructing effective various kinds of 2d and 3d optical lattices using laser beams and then load either ultra-cold fermion or boson atoms at different filling factors on the lattices. They may tune the parameters in Eqn.1 to realize different phases and quantum phase transitions^{27,28}. The optical honeycomb lattice geometry Fig.1 and square lattice could be realized in future ultra-cold atomic experiments. The challenge is to achieve longer range interactions than the onsite interaction. Very exciting perspectives to achieve longer range interactions have been opened by recent experiments²⁹ on cooling and trapping of polar molecules. Being electrically or magnetically polarized, polar molecules interact with each other via long-rang anisotropic dipole-dipole interactions. Loading the polar molecules on a 2d optical lattice³⁰ with the dipole moments perpendicular to the trapping plane can be mapped to Eqn.1 with long-range repulsive interactions $\sim p^2/r^3$ where p is the dipole moment. There are also other ways to generate long-range interactions³¹. We expect Fig.2a can be easily realized. There could also be some efficient ways to generate the ring exchange interactions³¹ needed to stabilize the the VBS state in Fig.2b.

VIII. ADATOM ADSORPTIONS ON SUBSTRATES (HONEYCOMB LATTICE)

In this section, we will use the phase diagram Fig.2a to discuss two experimental systems: (1) the reentrant "superfluid" detected in a narrow region of coverages in the second layer of He4 (called ${}^4\text{He}/{}^4\text{He}/\text{graphite}$ system) adsorbed on graphite by a previous torsional oscillator experiment (³⁸. (2) the reentrant "fluidlike" state of hydrogen adsorbed on Krypton-preplated graphite ($H_2/\text{Kr}/\text{graphite}$) near half filling which was investigated in a recent experiment⁴⁰.

The dual vortex approach is a Magnetic Space Group (MSG) symmetry based approach which can be used to classify all the possible phases and phase transitions.

However, the question if a particular phase will appear or not as a ground state depends on the specific values of all the possible parameters in the boson Hubbard model in Eqn.1, namely, the specific values in the real systems, it can not be addressed in this approach. There are two ways to remedy this short-coming. (1) we can compare our theoretical classifications with some known phases observed in experiments, then we can be more specific on our predictions on the nature of *unknown* phases and phase transitions. (2) As said in section VI, a microscopic approach such as Quantum Monte-Carlo (QMC) may be needed to supplement the dual field theoretical approach. In this section, we will take the first strategy to study the boson Hubbard model Eqn.1 in honeycomb lattice Fig.1 near $q = 2$ (Fig.1). The honeycomb lattice in Fig.1 may describe the preferred adsorption sites in the two systems. So the ${}^4\text{He}/{}^4\text{He}/\text{graphite}$ and $D_2/\text{Kr}/\text{graphite}$ systems may have the same symmetry and belong to the same universality class.

A. ${}^4\text{He}/{}^4\text{He}/\text{graphite}$ system

A superfluid is a fluid that flows through the tiniest channels or cracks without viscosity. So far, the phenomenon of superfluidity has been firmly observed in only two kinds of systems. The first system is the two isotopes of Helium: ${}^4\text{He}$ and ${}^3\text{He}$. ${}^4\text{He}$ is a boson and becomes a superfluid when $T < T_c = 2.18\text{K}$, while ${}^3\text{He}$ is a fermion, two ${}^3\text{He}$ atoms start to pair up when $T < T_c = 2.4\text{mK}$ and form a superfluid^{32,33}. The second system is Bose-Einstein condensation in ultra-cold alkali atomic gases (for a review, see²⁸). Recently, intensive research activities have been lavished on searching for excitonic superfluid in excitons in electron-hole semiconductor bilayers³⁴. Torsional oscillator method was used to study ${}^4\text{He}$ films adsorbed on graphite³⁸, a large Non-Classical Rotational Inertial (NCRI) was detected in a narrow window of coverages $c = 17 \sim 19 \text{ atoms}/\text{nm}^2$ in the second layer (${}^4\text{He}/{}^4\text{He}/\text{graphite}$ system). The NCRI is a low temperature reduction in the rotational moment of inertia due to the superfluid component of the state. This important phenomenon was interpreted as reentrant "superfluid" in this narrow window³⁹. Recently, also by using the torsional oscillator measurement, a PSU group lead by Chan observed a marked $1 \sim 2\%$ NCRI even in bulk solid ${}^4\text{He}$ at $\sim 0.2\text{K}$ ⁸. This was interpreted as a new state of matter called supersolid which has both superfluid order and crystalline order⁸. However, so far, no NCRI in bulk solid H_2 was detected.

At the completion of the first layer, the ${}^4\text{He}$ atoms with the coverage $c \sim 12 \text{ atoms}/\text{nm}^2$ form a triangular lattice which is incommensurate with the underlying graphite. It is reasonable to assume the lattice structure of the preferred adsorption sites on the second layer form a honeycomb lattice (Fig.1). When applying the Eqn.1 to the ${}^4\text{He}/{}^4\text{He}/\text{graphite}$ system in Fig.1, b_i^\dagger is the ${}^4\text{He}$ atom creation operator. The hopping amplitude t is de-

termined by the trapping potential from the incommensurate first ${}^4\text{He}$ layer. We assume the ${}^4\text{He}$ atoms interact with each other with the LJ potential. Note that the LJ potential is quite accurate in describing the long distance attractive part, but very crude in the short distance repulsive part. The repulsive part in real case is expected to be softer. The chemical potential μ determines the coverage. The filling factor f is related to the coverage c of ${}^4\text{He}$ with $c \sim 19.55 \text{ atoms}/\text{nm}^2$ corresponding to $f = 1/2$ where one ${}^4\text{He}$ atoms occupies every two lattice sites of the honeycomb lattice (for example, all the A sublattice sites) to form a close packed triangular lattice with $d_{AA} \sim 4.56\text{\AA}$ and $d_{AB} \sim 2.63\text{\AA}$ which is just smaller than Lennard-Jones (LJ) parameter $\sigma({}^4\text{He}) \sim 2.64\text{\AA}$. The onsite U is very big. Because $d_{AB} < \sigma_{{}^4\text{He}} < d_{AA}$, V_1 is positive, while V_2 and further neighbor interactions are weakly attractive and can be neglected. Note that our theoretical value $19.55 \text{ atoms}/\text{nm}^2$ is only 3% away from the experimental value $19 \text{ atoms}/\text{nm}^2$. Fig.2a is very similar to the ρ_s versus $c \sim f$ phase diagram in ${}^4\text{He}/{}^4\text{He}/\text{graphite}$ structure near $c = 19 \text{ atoms}/\text{nm}^2$ (see Fig. 1 in³⁸). The dashed line is the experimental path in ${}^4\text{He}/{}^4\text{He}/\text{graphite}$ at $T = 0$. It shows that a reentrant supersolid (SS) state is a generic state sandwiched between the C-IC transition. The reentrant "superfluid" state in the second layer of the ${}^4\text{He}$ films adsorbed on graphite could be a ${}^4\text{He}$ supersolid state. Very interestingly, the data in the torsional oscillator experiment in³⁸ do not show the characteristic form for a 2d ${}^4\text{He}$ superfluid film, instead it resemble that in⁸ characteristic of a possible supersolid in terms of the gradual onset temperature of the NCRI, the unusual temperature dependence of T_{SS} on the coverage. From Fig.2a, it is easy to see that it maybe difficult to reach the superfluid by moving along the horizontal r axis, but it is very easy to get to the CDW-SS state by moving along the vertical coverage axis. In principle, there should be a Kosterlitz-Thouless (KT) finite temperature phase transition above which the CDW-SS becomes a coexistence of the CDW state and normal fluids of interstitials. The effects of disorders on this finite temperature transition will be studied in and compared with Fig.2 and 3 in³⁸.

B. $\text{H}_2/\text{Kr}/\text{graphite}$ system

There are great interests in finding superfluidity in other substances. Hydrogen molecules are relatively light, quantum fluctuations are large at very low temperature. a para- H_2 molecule is a boson and very similar to a He_4 atom, in principle, H_2 could become superfluid at low temperature as He_4 does. Unfortunately, unlike He_4 , due to deeper attractive potentials, bulk H_2 solidifies at low temperature ($T_c \sim 14\text{K}$), this preempts the possible observation of the speculated superfluidity. At sufficiently high pressure, the solid hydrogen will transform into a metallic alkali-like crystal or an unusual two component (protons and electrons) quantum liquid at low

temperatures³⁷. Potential avenues to prevent p - H_2 from being solidified to low enough temperature such that the superfluid behaviour can be observed is by decreasing the average number of neighbors of a H_2 molecule. Monte Carlo simulations of H_2 clusters with $n = 13 - 18$ showed that there is indeed a tendency for the system to be superfluid below 1K³⁵. Indeed, Infra-red spectroscopy also provided evidences for superfluidity in $o(D_2)_n$ and $p(H_2)_n$ clusters with $n = 14 - 17$ ³⁶. Another route is by the reduction of dimensionality. Extensive theoretical and experimental work has been devoted to study H_2 and D_2 films in a variety of substrates. Path Integral Monte-Carlo (PIMC) simulations indicated that introduction of certain impurities can stabilize a 2 dimensional liquid hydrogen which undergoes a Kosterlitz-Thouless (KT) transition below 1.2 K.

In a recent experiment, neutron scattering measurements were used to characterize all the possible phases of D_2 coadsorbed on graphite preplated by a monolayer of Kr called D_2 /Kr/graphite structure⁴⁰. Because two dimensional graphite has the honeycomb net structure, the corresponding preferred adsorption sites form a triangular lattice. The precoated Kr atoms will occupy the preferred adsorption sites and form a triangular lattice. Then the D_2 deposited on top of the Kr monolayer will sit on the preferred adsorption sites of the triangular lattice of the Kr monolayer to form a honeycomb lattice. So, the lattice geometry is very similar to Fig.1 with Kr atoms sitting on the triangular lattice, while the H_2 molecules hopping on the honeycomb lattice. The filling factor f is related to the coverage c of D_2 . In the coverage c verse the temperature T phase diagram, an unusual feature is that in a small coverage range ($1.20 < c < 1.25$) at the commensurate-incommensurate (C-IC) transition, a reentrant *fluid* phase squeezes in between the C and IC phases down to $T = 1.5$ K which is the lowest temperature a liquidlike phase of D_2 has ever been found. The filling factor f is related to the coverage c of H_2 with $c = 1.2$ corresponding to $f = 1/2$ where one H_2 molecule occupies every two lattice sites of the honeycomb lattice with $d_{AA} \sim 3.87\text{\AA}$ and $d_{AB} \sim 2.24\text{\AA}$ in Fig.1. Because $d_{AB} < \sigma_{H_2} < d_{AA}$, V_1 could also be positive and very big, while V_2 and further neighbor interactions are weakly attractive, the above discussions on 4He in subsection A can also be applied to this system. Fig.2a is very similar to the $c \sim f$ versus low T phase diagram in H_2 /Kr/graphite structure near $c = 1.20$ (Fig. 6 in⁴⁰). The dashed line is the experimental path in H_2 /Kr/graphite at $T = 0$. The so called $(1 \times 1)_{[1/2]}$ commensurate phase in⁴⁰ is the CDW state where the D_2 atoms occupy one of the two sublattices of the underlying honeycomb lattice. The transition at zero temperature is a C-CDW to CDW-SS to IC-CDW transition described by Fig.2(a). The first transition is in the $z = 2, \nu = 1/2, \eta = 0$ universality class. Because $\nu < 1$, from Harris criterion, disorders are relevant. The second transition is first order. It suggests the reentrant "fluidlike" phase could be the H_2 supersolid. If this is

indeed the case, this may lead to the first observation of H_2 supersolid. Torsional oscillator experiment similar to that used in³⁸ may be used to measure the NCRI of this H_2 supersolid state. Obviously, this experiment can avoid the difficulty of using D_2 which has large coherent neutron scattering cross section, but smaller de Boer quantum number. In fact, Kr may not be the best spacer to observe the H_2 supersolid state. The ideal situation is to make d_{AB} is just slightly smaller than σ_{H_2} . Larger atoms like Xe, CF_4, SF_6 may be more suitable spacers, because they may increase the distance d_{AB} in the Fig.1 just slightly smaller than σ_{H_2} . We suggest that 4He supersolid should also appear in, for example, 4He /Kr/graphite structure.

The reentrant lattice SS discussed in this section is different from the bulk 4He SS state discussed in⁹, although both kinds of supersolids share many interesting common properties. In the former, there is a periodic substrate or spacer potential which breaks translational symmetries at the very beginning. While in the latter, the lattice results from a spontaneous translational symmetry breaking, so the theory developed in this paper on lattices is completely different from the continuum theory developed in⁹. Combined with the results in⁹, we conclude that 4He supersolid can exist both in bulk and on substrate, while although H_2 supersolid may not exist in the bulk, but it may exist on wisely chosen substrates. Ultra-cold atoms supersolid could also be realized in optical lattices.

IX. COOPER-PAIR SOLID, SUPERFLUID AND COOPER-PAIR SUPERSOLID IN HIGH TEMPERATURE SUPERCONDUCTORS (SQUARE LATTICE)

Very recently⁴¹, by using both angle resolved photoemission (ARPES) and scanning tunneling microscopy (STM) on high temperature superconductor $La_{2-x}Ba_xCuO_4$ ^{42,43}, Valla *et.al* detected a quasi-particle energy gap with d -wave symmetry even when the superconductivity is completely suppressed at $x = 1/8$, while having almost equally strong superconducting phases at both higher and lower dopings (Fig.5). The gap turns out to reach maximum at $x = 1/8$ despite $T_c \rightarrow 0$ at $x = 1/8$. This fact suggests that the most strongly bound Cooper pairs at $x = 1/8$ are most susceptible to the charge density wave (CDW) ordering which suppresses $T_c \rightarrow 0$. In this section, I propose that the formation of a stripe Cooper pair supersolid may be able to explain the very unusual phase diagram of $La_{2-x}Ba_xCuO_4$ at and near doping level $x = 1/8$.

The fact that the STM and ARPES measurements in⁴¹ still detected an energy gap at Fermi surface with $d_{x^2-y^2}$ wave symmetry suggests that there are tightly bound Cooper pairs in this cuprate. We can treat these Cooper pairs as bosons, therefore many important results achieved in previous sections on interacting bosons

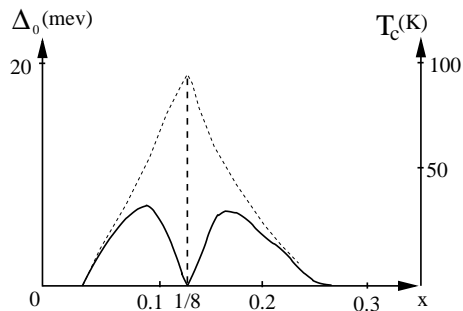


FIG. 5: The dashed line is the energy gap Δ_0 which reaches minimum at $x = 1/8$, the solid line is the superconducting transition temperature T_c which has two domes and is zero at $x = 1/8$.

hopping on lattices maybe applied to this cuprate. One important new feature for tightly bound Cooper pairs is that they carry charges $2e$, therefore interact with bare long-range Coulomb interaction (in high T_c cuprates, by taking the penetration depth $\lambda \rightarrow \infty$, one can neglect the very weak Meissner effect)³. I propose the following physical picture: at exactly $x = 1/8$, the filling factors of the bosons on the square lattice is $f = \frac{1-x}{2} = 7/16$, the system is a CDW (more specifically, stripe) of Cooper pairs with 4 sites per unit cell, so $T_c = 0$. Then we need $q = 16$ dual vortices to describe the stripe CDW in the dual vortex picture. It was explicitly pointed out in section III that special care is needed to choose the correct saddle point of the dual gauge field A_μ to describe this stripe CDW state. *Slightly away from $x = 1/8$, on both sides, the groundstate is a Stripe Cooper pair supersolid (CP-SS) !* When $x > 1/8$ ($x < 1/8$), it is a hole (electron) doped stripe CP-SS. Indeed, as shown by Quantum Monte-Carlo simulation¹⁴, only striped supersolid is stable in a square lattice for hardcore bosons. The quantum phase transition from the stripe Cooper pair solid to the stripe CP-SS driven by the doping is in the same universality class as that from a Mott insulator to a superfluid, therefore have exact exponents $z = 2, \nu = 1/2, \eta = 0$ (with possible logarithmic corrections). The resulting stripe CP-SS has *the same lattice symmetry breaking patterns* as the stripe Cooper pair solid with the superfluid density scaling as $\rho_s \sim |x - 1/8|^{(d+z-2)\nu} = |x - 1/8| = |\delta x|$ with a possible logarithmic correction. As pointed out in section III, the superfluid density is anisotropic with ρ_s along the stripe is larger than that normal to the stripe, but both scale in the same way with different coefficients. From Uemura relation, we conclude that $T_c \sim |\delta x|$ (in fact, it scales as the smaller ρ_s in the Stripe CP-SS). This result very naturally explains why T_c indeed looks linear in $|\delta x|$ and the phase diagram is nearly symmetric near $x = 1/8$ found in⁴¹.

The above picture only involves the sector of the tightly bound Cooper pair. Of course, understanding the ground state of the Cooper-pair sector is very important

on its own and is also the starting point to incorporate quasi-particles^{45,46,47} and spin excitations⁴⁸ into the picture. As shown in section IV, a valence-bond supersolid (VB-SS) can be stabilized if there is a considerable ring exchange interaction. An interesting question to address is if valence-bond Cooper-pair supersolid can be realized in some of these cuprates.

X. CONCLUSIONS

By using the DVM, we studied superfluid, solid and supersolid and quantum phase transitions of the extended boson Hubbard model near half filling on bipartite optical lattices such as honeycomb and square lattice and mapped out the global phase diagram at $T = 0$ in a unified scheme. We identified boson density and boson kinetic energy operators in terms of the dual vortex fields to characterize symmetry breaking patterns in the insulating states and supersolid states. In the DVM, starting from the featureless superfluid state where the the average value of the dual gauge field through a dual plaquette is taken to be uniform and equal to the boson density $f = p/q$, its fluctuation is coupled to q dual vortex order parameters and is gapless, one study all the possible symmetry breaking patterns by condensing the q vortex order parameters. We first study the transition driven by the ratio of the kinetic energy over the potential energy at the commensurate fillings $f = p/q$ along the horizontal axis in Fig.2-4. In the Ising limit, we found that the saddle point of the dual gauge fields should be chosen in a self consistent way in the CDW side, this is in sharp contrast to the more familiar $f = n$ case where the self-consistency condition is automatically guaranteed. Due to this change of saddle point structure of the dual gauge fields on the both sides, the SF to the CDW transition is always a strong first order one. In the Easy-plane limit, we found that the self-consistency condition is automatically guaranteed, the SF to the VBS transition is a weak first order one. Then we study the transition driven by chemical potential slight away from the commensurate fillings $f = p/q$ along the vertical axis in Fig.2-4. We found that in the insulating side, the transition at zero temperature driven by the chemical potential must be a C-CDW (or C-VBS) at half filling to a narrow window of CDW- (VB-) supersolid, then to a IC-CDW (IC-VBS) transition in the Ising (easy-plane) limit. The valence bond supersolid is a novel kind of supersolid first proposed in this paper. Although the density fluctuation at *any site* is very large indicating its superfluid nature, the boson *kinetic energies on bonds* between two sites are given and break the lattice translational symmetry indicating its valence bound nature. The first transition is in the same universality class as that from a Mott insulator to a superfluid driven by a chemical potential, therefore have exact exponents $z = 2, \nu = 1/2, \eta = 0$ with a logarithmic correction. The second is a 1st order transition. The results achieved in this letter could guide

QMC simulations to search for all these phases and confirm the universality class of the transitions. This VB-SS should be stable in both hard core and soft core limit if there is a sufficient strong ring exchange term in Eqn.1. It will be extremely interesting to search this novel kind of supersolid in a specific microscopic model by QMC simulation.

In the second part of this paper, we study the applications of the results achieved in the first part by the DVM to 3 very important ultra-cold atomic and condensed matter experimental systems. The EBHM in honeycomb and square lattices could be realized in ultracold atoms loaded on optical lattices. So the results achieved in this paper may have direct impacts on the atomic experiments in optical lattices. Then we applied the results to two condensed matter experimental systems: (1) adatom adsorption on different substrates such as the adsorption in the second layer of ${}^4\text{He}$ adsorbed on graphite and Hydrogen adsorbed on Krypton-preplated graphite in honeycomb lattice, we find that a reentrant ${}^4\text{He}$ supersolid in the second layer on graphite may be responsible for the NCRI detected in the torsional oscillator experiments in³⁸ and a reentrant H_2 supersolid at $T = 0$ maybe responsible for the reentrant liquid state squeezed between C and IC phases detected by coherent neutron scattering. We propose that a judicious choice of substrate may also lead to an occurrence of hydrogen lattice supersolid. (2) superconducting phase diagram near $x = 1/8$ in high temperature superconductor $\text{La}_{2-x}\text{Ba}_x\text{CuO}_4$ in square lattice. We conclude that there is a stripe CDW at $1/8$ which suppresses T_c to zero. There are hole and electron doped Cooper pair supersolids on both sides of $x = 1/8$ which has the same lattice symmetry breaking pattern as the stripe CDW at $x = 1/8$ and with $\rho_s \sim T_c \sim |x - 1/8|$. Although the SS in lattice models is different from that in a continuous systems, the results achieved in this paper on lattice supersolids may still shed some lights on the possible microscopic mechanism and phenomenological Ginsburg-Landau theory of the possible ${}^4\text{He}$ supersolids⁹.

I thank Milton Cole for pointing out the experiment in Ref.⁴⁰ to me. I also like to thank A. Millis for pointing out Ref.⁴¹ to me and helpful discussions. This research at KITP was supported in part by the NSF under Grant No. PHY99-07949 at KITP-C by the Project of Knowledge Innovation Program (PKIP) of Chinese Academy of Sciences. I also thank C.P. Sun for hospitality during my visit at KITP-C.

APPENDIX A: DUALITY AT INTEGER FILLINGS $f = n$, THE ROLE OF THE DUAL GAUGE FIELD AND THE SELF-CONSISTENCY CONDITION

It is instructive to review the direct boson picture and the duality transformation to the dual vortex picture in this simplest case with integer filling $f = n^4$. The con-

tents of this appendix are not new. However, we stress the self-consistence check on the average value of the dual magnetic field on both sides of SF and Mott insulator. We also explicitly spell out the physical significance of the fluctuations of the dual gauge field on both sides. These clarifications are very helpful to motivate the self-consistence condition on the average value of the dual magnetic fields in the translational symmetry breaking insulating sides, especially in the CDW side at $q \geq 2$ cases first discovered in¹⁰. Although this self-consistence condition is automatically satisfied at $f = n$ case, they become a non-trivial constraint on a self-consistent theory at $q \geq 2$ cases. In a recent unpublished note⁵⁰, the author found this self-consistent condition is even more non-trivial and important in frustrated lattices such as triangular and Kagome lattices than the bipartite lattices discussed in this paper. As shown in the main text, in both the CDW side (using limit) and the valence bond (easy plane limit), at and slightly away from the commensurate filling $f = p/q$ with $q \geq 2$ cases, the effective actions can be mapped to Eqn.A2 and Eqn.A4.

In the direct picture, it is convenient to start from the Mott insulating side and look at its low energy excitations, it is easy to see that the creation of a particle by ϕ^\dagger is always accompanied by a creation of a hole ϕ due to the particle hole symmetry at $f = n$, so the Ginsburg-Landau theory to describe the Mott to superfluid transition in terms of the boson order parameter ϕ is given by the well know $2 + 1$ dimensional relativistic complex scalar theory:

$$\mathcal{S}_b = \int d^2r d\tau [|\partial_\tau \phi|^2 + |\nabla \phi|^2 + r|\phi|^2 + u|\phi|^4 + \dots] \quad (\text{A1})$$

In the Mott state $r > 0$, so $\langle \phi \rangle = 0$, there is a Mott gap. In the superfluid state $r < 0$, so $\langle \phi \rangle \neq 0$. Due to the symmetry breaking in the SF state, there is a gapless goldstone mode given by the phase fluctuation of ϕ .

In the dual vortex picture, it is convenient to start from the Superfluid side and look at its low energy excitations. There are two kinds of low energy excitations. The first is just the gapless Goldstone mode in the phase of ϕ which is given by a dual gauge field fluctuation A_μ . The second is the topological vortex excitation in the phase winding of ψ . Obviously, the number of vortex ψ^\dagger is equal to the number of anti-vortex ψ , so the Ginsburg-Landau theory to describe the superfluid to the Mott transition in terms of the dual vortex order parameter ψ is given by the $2 + 1$ dimensional scalar electrodynamics:

$$\mathcal{S}_d = \int d^2r d\tau [|(\partial_\mu - iA_\mu)\psi|^2 + r_d|\psi|^2 + u_d|\psi|^4 + \dots + \frac{1}{4}(\epsilon_{\mu\nu\lambda}\partial_\nu A_\lambda)^2] \quad (\text{A2})$$

In the superfluid state $r_d > 0$, so $\langle \psi \rangle = 0$, there is a gapless fluctuation given by the dual gauge field A_{μ} . Integrating out the gauge field fluctuation A_μ will lead to a logarithmic interaction between the vortices. In the

Mott insulating state $r_d < 0$, so $\langle \psi \rangle \neq 0$. Due to the "symmetry" breaking in the Mott insulating state, the dual gauge field A_μ acquires a mass due to Higgs mechanism, so there is a Mott gap in the Mott phase. The vortex action Eqn.A2 is dual to the boson action Eqn.A1. Both actions lead to equivalent description of the SF to Mott transition which is in the $3DXY$ universality class and the same excitation spectra in both phases. Indeed, this universality class has been confirmed by QMC in the first reference in⁴ from both the direct boson action Eqn.A1 and the dual vortex action Eqn.A2.

In the direct boson picture, a vortex is a singularity in the boson wavefunction, so a boson wavefunction acquires a 2π phase when it encircles a vortex. In the dual vortex picture, a boson is a singularity in the vortex wavefunction, so a vortex wavefunction acquires a 2π phase when it encircles a boson. So the average strength of the dual magnetic field of the gauge field A_μ through a dual plaquette is equal to the boson density $f = n$, because $2\pi n$ is equivalent to 0, so the average value can be simply taken to be zero. It is important to stress that the average density of bosons is the same in both the SF and the Mott insulating side, namely, it takes the integer n on both sides, so the average strength of the dual magnetic field can be taken as zero on both side, then the fluctuations in the dual gauge field reflects the fluctuations of the boson density. As said in the last paragraph, the gauge field is gapless in the SF phase, so the boson density fluctuation in the SF is very large, this is expected, because the SF is a phase ordered state, so it has a large density fluctuation. However, in the Mott phase, the gauge field is massive, so the density fluctuation is suppressed in the Mott phase. This is expected also, because the Mott phase is a density ordered phase, so has very little density fluctuations. So by looking at the behaviors of

the dual gauge field on both sides, one can distinguish the properties of the two phases. In short, although the average value of the dual gauge field is the same on both the SF and the Mott insulating side, its fluctuations are completely different which, in turn, is determined by the average value of the vortex order parameter ψ in Eqn.A2.

When slightly away from $f = n$ which is at a incommensurate density, there is no particle-hole symmetry anymore, so there should be a first order imaginary time derivative, Eqn.A1 becomes:

$$\mathcal{S}_{ic-b} = \int d^2 r d\tau [\phi^\dagger \partial_\tau \phi + |\nabla \phi|^2 + r|\phi|^2 + u|\phi|^4 + \dots] \quad (\text{A3})$$

where we have dropped the second derivative term $|\partial_\tau \phi|^2$ which is less important than the linear derivative term. If there is only a onsite interaction in Eqn.1, then away from $f = 1$, the system is always in the superfluid state. The transition from the Mott to the SF transition driven by the chemical potential has the critical exponents $z = 2, \nu = 1/2, \eta = 0$ with a logarithmic correction.

In the dual vortex picture, the linear time derivative term corresponds to adding a small mean dual magnetic field $\delta f = f - n$ to Eqn.A2:

$$\mathcal{S}_{ic-d} = \int d^2 r d\tau [|(\partial_\mu - iA_\mu)\psi|^2 + r_d|\psi|^2 + u_d|\psi|^4 + \dots + \frac{1}{4}(\epsilon_{\mu\nu\lambda} \partial_\nu A_\lambda - 2\pi \delta f \delta_{\mu\tau})^2] \quad (\text{A4})$$

This action is essentially the same as the Ginzburg-Landau model for a superconductor in a external magnetic field if we identify the τ direction as the \hat{z} direction along which the magnetic field δf is applied. For a type II superconductor, its phase diagram is shown in Fig.2a.

-
- ¹ M. P. A. Fisher, P. B. Weichman, G. Grinstein and D. S. Fisher; Phys. Rev. B 40, 546 (1989).
² M. P. A. Fisher and G. Grinstein, Phys. Rev. Lett. 60, 208 (1988).
³ Jinwu Ye, Phys. Rev. B 58, 9450-9459 (1998).
⁴ C. Dasgupta and B. I. Halperin, Phys. Rev. Lett. 47, 1556-1560 (1981), David R. Nelson, Phys. Rev. Lett. 60, 1973-1976 (1988); Matthew P. A. Fisher and D. H. Lee, Phys. Rev. B 39, 2756-2759 (1989).
⁵ L. Balents, *et.al* Phys. Rev. B 71, 144508 (2005).
⁶ Douglas R. Hofstadter, Phys. Rev. B 14, 2239-2249 (1976).
⁷ J. Zak, Phys. Rev. 134, A1602-A1606 (1964), Phys. Rev. 134, A1607-A1611 (1964).
⁸ E. Kim and M. Chan, Science 24, 1941 (2004).
⁹ Jinwu Ye, Phys. Rev. Lett. 97, 125302 (2006), Europhysics Letters, 82 (2008) 16001; cond-mat/0603269.
¹⁰ Jinwu Ye, cond-mat/0503113.
¹¹ Longhua Jiang and Jinwu Ye, J. Phys, Condensed Matter. 18 (2006) 6907-6922.
¹² G. Murthy, D. Arovas, A. Auerbach, Phys. Rev. B 55, 3104 (1997).
¹³ G. C. Batroun *et al*, Phys. Rev. Lett. 74, 2527 (1995); *ibid*, 84, 1599 (2000).
¹⁴ F. Hebert, *et al*; Phys. Rev. B, 65, 014513 (2001).
¹⁵ P. Sengupta, *et al*, Phys. Rev. Lett. 94, 207202 (2005).
¹⁶ P.W. Anderson; Science 235, 1196(1987); N. Read and S. Sachdev, Phys. Rev. Lett. 62, 1694 (1989); Phys. Rev. B42, 4568 (1990).
¹⁷ The discussions in the following equally apply to the striped solid with $(\pi, 0)$ or $(0, \pi)$ order with the exception of the anisotropy in the superfluid density. The anisotropy is irrelevant to the universality class.
¹⁸ In the direct lattice picture, we can simply renormalize away the sublattice A where the bosons sit and focus on the effective boson hopping on the sublattice B whose dual vortex action is given by Eqn.19. If δf is replaced by $-\delta f$, then the b index should be replaced by the a index, the vortices in the phase winding of ψ_a should be interpreted as the vacancy number.
¹⁹ D. S. Fisher, M. P. A. Fisher and D. A. Huse, Phys. Rev. B 43, 130 (1991).
²⁰ Jing Yu Gan, Yu Chuan Wen, Jinwu Ye, Tao Li, Shi-Jie

- Yang, Yue Yu, Phys. Rev. B 75, 214509 (2007).
- ²¹ Jinwu Ye, Phys. Rev. B 67, 115104 (2003); J. Phys. Condens. Matter 16 (2004) 4465-4476.
- ²² In quantum impurity problems, in the scaling limit, the impurity degree of freedoms disappear and are replaced by operators with the same symmetry, see, for example, Jinwu Ye ; Phys. Rev. Lett. 79, 1385 (1997).
- ²³ In principle, the δf should be the chemical potential.
- ²⁴ Similar quantum phase transitions induced by bias volatge may appear in im-balanced Bi-layer Quantum Hall systems at total filling factor $\nu_T = 1$, Jinwu Ye, Phys. Rev. Lett. 97, 236803 (2006). Although the results achieved in this paper are correct, the the change of saddle point structures of the dual gauge fields was not recognized. This fact was clarified in Jinwu Ye, Annals of Physics, 323 (2008), 580-630.
- ²⁵ O.I. Motrunich and A. Vishwanath, Phys. Rev. B 70, 075104 (2004); T. Senthil, Ashvin Vishwanath, Leon Balents, Subir Sachdev, M. P. A. Fisher, Science 303, 1490 (2004); cond-mat/0312617.
- ²⁶ A. Kuklov, N. Prokof'ev, B. Svistunov, Matthias Troyer, cond-mat/0602466.
- ²⁷ M. Greiner, *et al*, Nature 415, 39-44 (2002).
- ²⁸ F. Dalfovo, S. Giorgini, L. P. Pitaevskii and S. Stringari, Rev. Mod. Phys. 71, 463C512 (1999).
- ²⁹ Jeremy M. Sage, Sunil Sainis, Thomas Bergeman, and David DeMille, Phys. Rev. Lett. 94, 203001 (2005), T. Rieger, T. Junglen, S. A. Rangwala, P. W. H. Pinkse, and G. Rempe, Phys. Rev. Lett. 95, 173002 (2005). M. A. Baranov, Klaus Osterloh and M. Lewenstein, Phys. Rev. Lett. 94, 070404 (2005). J. Stuhler, A. Griesmaier, T. Koch, M. Fattori, T. Pfau, S. Giovanazzi, P. Pedri, and L. Santos, Phys. Rev. Lett. 95, 150406 (2005).
- ³⁰ K. Gral, L. Santos, and M. Lewenstein, Phys. Rev. Lett. 88, 170406 (2002).
- ³¹ H. P. Bchler, M. Hermele, S. D. Huber, Matthew P. A. Fisher, and P. Zoller, Phys. Rev. Lett. 95, 040402 (2005).
- ³² P. Kapitza, Nature 141, 74 (1938).
- ³³ D. D. Osheroff, R. C. Richardson, and D. M. Lee, Phys. Rev. Lett. 28, 885C888 (1972)
- ³⁴ Jinwu Ye, arXiv:0712.0437.
- ³⁵ P. Sindzingre, D. M. Ceperley and M. L. Klein, Phys. Rev. Lett. 67, 1871C1874 (1991).
- ³⁶ Slava Grebenev, Boris Sartakov, J. Peter Toennies, and Andrei F. Vilesov, Science 1 September 2000; 289: 1532-1535
- ³⁷ Stanimir A. Bonev, Eric Schwegler, Tadashi Ogitsu, Giulia Galli, Nature 431, 669 - 672 (07 Oct 2004).
- ³⁸ P. A. Crowell and J. D. Reppy, Phys. Rev. Lett. 70, 3291C3294 (1993); Phys. Rev. B 53, 2701C2718 (1996).
- ³⁹ The possibility of supersolid was briefly mentioned in the second reference in³⁸. P. A. Crowell and J. D. Reppy, private communications.
- ⁴⁰ Horst Wiechert and Klaus-Dieter Kortmann, Norbert Ster, Phys. Rev. B 70, 125410 (2004).
- ⁴¹ T. Valla, A. V. Fedorov, Jinho Lee, J. C. Davis, G. D. Gu, Vol. 314. no. 5807, pp. 1914 - 1916. Science 22 December 2006.
- ⁴² J. G. Bednorz and K. A. Muller, Z. Phys. B 64, 189 (1986)
- ⁴³ A. R. Moodenbaugh, Youwen Xu, and M. Suenaga, T. J. Folkerts and R. N. Shelton, Phys. Rev. B 38, 4596 - 4600 (1988).
- ⁴⁴ J. M. Tranquada, H. Woo, T. G. Perring, H. Goka, G. D. Gu, G. Xu, M. Fujita, K. Yamada, Nature 429, 534 - 538 (03 Jun 2004).
- ⁴⁵ Jinwu Ye and S. Sachdev, Phys.Rev.B, 10173 (1991).
- ⁴⁶ Jinwu Ye, Phys. Rev. Lett. 86, 316 (2001).
- ⁴⁷ Jinwu Ye, Phys. Rev. Lett. 87, 227003 (2001).
- ⁴⁸ A. V. Chubukov, S. Sachdev and Jinwu Ye, Phys. Rev. B 49, 11919 (1994).
- ⁴⁹ Christopher P. Herzog, Pavel Kovtun, Subir Sachdev and Dam Thanh Son, Phys. Rev. D 75, 085020 (2007).
- ⁵⁰ In a very recent preprint on Kagome lattice, Jinwu Ye, arXiv:0804.3429, unpublished, it was found that a simily action in Ising limit indeed describes a first order transition from the SF to a trinagulat valence bond state.